32nd URSI GASS, Montreal, 19-26 August 2017

Application of Electromagnetic Models for Sea Near-Surface Wind Speed Retrieval from C-Band SAR Images

Tran Vu La[1], Ali Khenchaf[1], Fabrice Comblet[1], and Carole Nahum[2]
(1) ENSTA Bretagne, 29806 Brest Cedex 09, France, www.ensta-bretagne.fr
(2) Direction générale de l'armement (DGA), 75509 PARIS Cedex 15, France

Abstract

Synthetic Aperture Radar (SAR) is one of the favorite sources for sea near-surface wind speed retrieval. For this problem, wind speed is principally estimated based on the empirical (EP) models, namely CMOD functions, which are constructed by the observations from spaceborne microwave scatterometers (ERS-1/2). Little studies have mentioned the use of electromagnetic (EM) models for wind speed estimation, probably due to their complicated descriptions. However, it is reasonable to compare wind speed estimates based on the two approaches, since both of them describe the relation of radar scattering and wind field, directly for EP models and via wave surface roughness for EM models. Based on the comparisons, some ideas are proposed to improve the performance of EP and EM models.

1. Introduction

Sea near-surface wind is an important factor for the studies of oil spill propagation, ship detection, marine weather prediction, etc. In particular, wind speed and wind direction are the crucial parameters for the calculation of radar scattering from sea surface, since it influences significantly the formation of wave surface roughness. Among available wind sources, *i.e.* marine buoy data, numeric weather prediction model, Synthetic Aperture Radar (SAR) is a favorite one to obtain wind parameters, since it can offer the data at a high spatial resolution and in most meteorological conditions. For wind speed retrieval, in spite of many proposed studies in recent years, *i.e.* Doppler centroid [1], azimuth wavelength cut-off [2], the scatterometry approach [3-6] is still one of the most widely used methods, since it can estimate quite accurately wind speed from 2 to 25 m/s. For this approach, radar backscattering or normalized radar cross section (NRCS) is described as a function of wind speed, wind direction, radar incidence angle and radar look, namely Geophysical Model Function (GMF). Once wind direction is determined and the geometry of observation is known from SAR data, wind speed the 10-m reference height can be estimated by inverting the GMF. In C-band, one can find the GMF series, namely CMOD functions [3-6], which are developed based on observations from spaceborne microwave scatterometers (ERS-1/2). Therefore, they are also called the empirical (EP) GMF.

In constrast to EP GMF, in the electromagnetic (EM)-based approach, the relation between radar scattering and wind parameters via sea surface roughness is constructed based on the physical calculations of reflection and dispersion of radar signal on sea surface. Depending on different approaches, the EM models of radar scattering from sea surface can be constructed based on quasi-exact calculations, *i.e.* Method of Moment [7], Forward-Backward Method [8], or based on asymptotic method, *i.e.* Composite Two-Scale Model (CTSM) [9], Small-Slope Approximation (SSA) [10], and Resonant Curvature Approximation (RCA) [11]. For the range of 20°–60° incidence angle of most SAR systems, the EM models based on asymptotic method are more widely used since their descriptions are quite simpler, and then they can offer the results more rapidly, while the NRCS calculated by two approaches is quite similar. Among the EM models based on asymptotic method, the CTSM, SSA and RCA can describe sea surface roughness with multi-scale (large- and small-scale), while the SPM only calculates radar scattering from small-scale roughness. In other words, the domain of validity of the CTSM, SSA and RCA is larger than that of the SPM in terms of wind speed and incidence angle.

Although the EM models have not been developed for the inverse problem to estimate near-surface wind speed, it is reasonable to compare the EP and EM models since both of them describe the relation of radar scattering and wind field. Based on the comparisons of NRCS calculation and wind speed estimation for different scenarios of polarization and incidence angle, we can understand more clearly the difference between EP and EM GMF, and then some ideas can be proposed to improve their performance.

2. Electromagnetic Models

2.1 Composite Two-Scale Model (CTSM)

The CTSM [9] is constructed based on the combination of Kirchhoff Approximation (KA) and Small Perturbation Model (SPM) for the calculation of radar scattering from large-scale and small-scale surface roughness, respectively. In general, the CTSM can be described as

$$\sigma_{CTSM}^{s} = \sigma_{KA}^{s} + \int W\left(\frac{\vec{k}}{k_z}\right)\sigma_{SPM}^{s}\left(\vec{k} - 2\overrightarrow{k_H}\right)d\vec{k} \qquad (1),$$

where σ_{CTSM}^{s}, σ_{KA}^{s}, and σ_{SPM}^{s} are the normalized radar cross section (NRCS) calculated by the CTSM, KA and SPM, respectively; W is the probability density function (PDF) of the surface slope of the long wave portion of the surface; k_z is the z-component of the radar wavenumber vector k, and k_H is the projection of the 3-D k vector onto the horizontal surface.

The SPM [9], or Bragg mechanism, is constructed based on the principle of resonance between spatial wavenumber of ocean waves K and radar wavenumber k, which is described as $K = 2k_r \times \sin\theta$, where θ is the radar incidence angle. The general description of SPM can be illustrated as

$$\sigma_{pq}^{s} = 16\pi k_r^4 cos^4\theta\left|\alpha_{pq}(\theta)\right|^2 S(K, \Phi) \qquad (2),$$

where p and q denote transmitting and receiving polarizations (vertical V or horizontal H), α_{pq} is the scattering coefficients which relate to seawater permittivity or temperature and salinity, and $S(K, \Phi)$ is the directional surface roughness spectrum.

2.2 Small-Slope Approximation (SSA)

As well as CTSM, the SSA [10] is constructed based on the combination of KA and SPM for the calculation of radar scattering from multi-scale surface roughness. However, it calculates radar scattering by only one processing, without the intervention of division between the surface roughness structures. There are two versions of SSA: first-order (SSA-1) and second order (SSA-2). For scattering from ocean-like surfaces at microwave frequencies, the difference between two versions is relatively small. Therefore, we only present in this study the description of SSA-1 as

$$\sigma_{pq}^{s}(k, k_0) = \left|\frac{B_0(k,k_0)}{Q_z}\right|^2 \int e^{-Q_z^2[\rho(0)-\rho(r)]}\, e^{-iQ_H r} dr \qquad (3),$$

where $B_0(k, k_0)$ is the Bragg kernel, and $\rho(r)$ is the autocorrelation function of ocean waves.

2.3 Resonant Curvature Approximation (RCA)

The RCA [11] has been recently developed to improve the calculation of radar scattering in HH-pol. Its description is very close to that of SSA, but the Bragg kernel B_0 is replaced by the Kirchhoff kernel K_0, and the $\rho(r)$ function is modified to $\tilde{\rho}(r)$ by adding a kernel which is defined as $T_0 = B_0 - K_0$. The general equation of RCA is described as

$$\sigma_{pq}^{s}(k, k_0) = \left|\frac{K_0(k,k_0)}{Q_z}\right|^2 \int e^{-Q_z^2[\tilde{\rho}(0)-\tilde{\rho}(r)]}\, e^{-iQ_H r} dr \qquad (4)$$

3. Comparison with Empirical Model

3.1 CMOD Function

For the retrieval of near-surface wind speed in C-band, one can find the CMOD functions [3-6] which have a general form defined as

$$\sigma_{VV}^{s} = A[1 + b_1 \times \cos\Phi + b_2 \times \cos 2\Phi]^B \qquad (5),$$

where σ_{VV}^{s} is the vertical-polarized (VV-pol) NRCS of the ocean surface, Φ is the relative wind direction to radar look. The coefficients A, b_1, b_2 are described as the functions of wind speed at the 10 m reference height (U_{10}) and incidence angle θ. The exponent B is a fixed value. Among CMOD functions, the CMOD5.N [6] is a recently developed GMF for the correction of wind speed estimates from 1–25 m/s, and it is chosen in this paper for comparisons with the EM GMF. For the calculation of horizontal-polarized (HH-pol) NRCS, a polarization ratio (PR) [12-13] defined as in (6) is used. There are many models to calculate PR, depending on measured data. In this paper, we select the PR calculation proposed by Liu *et al.* [13].

$$PR = \frac{\sigma_{VV}^{0}}{\sigma_{HH}^{0}} \qquad (6).$$

3.2 NRCS Comparison

The NRCS calculated by the CMOD5.N, CTSM, SSA, and RCA as a function of wind speed is compared in Fig. 1. At θ = 20°, the NRCS level given by four studied GMF is quite similar. This is noted for both VV- and HH-pol. At θ = 30°, for VV-pol the CMOD5.N and SSA give quite similar results, while the level offered by the RCA is slightly lower, and the NRCS given by the CTSM is underestimated, especially for wind speed below 25 m/s. The similar result is noted at θ = 40°, but the deviation between CMOD5.N and EM GMF is more significant. Likewise, for HH-pol the NRCS level given by the EM GMF is lower than that of CMOD5.N. However, the RCA improves NRCS calculation for θ > 30°, while the deviation of NRCS between CMOD5.N, SSA and CTSM is more significant.

The poor performance of CTSM and SSA in NRCS calculation for θ > 30° in HH-pol has been expected, in spite of the change of surface roughness spectrum. The reason is that the contribution of small-scale wave breaking and foam to NRCS has not been considered in the description of CTSM and SSA. Since the HH-pol NRCS is smaller than that in VV-pol for θ > 30°, the contribution of wave breaking and foam is more significant for NRCS calculation in HH-pol. This is

clearly noted in Fig. 1. At $\theta = 20°$, the NRCS for VV-pol and HH-pol is very close, the CTSM, SSA and RCA offer quite similar NRCS to the CMOD5.N. However, for $\theta > 30°$ the deviation is larger. For the RCA, while NRCS calculation is clearly improved for $\theta < 40°$, the difference from the CMOD5.N is still more 3 dB for $\theta > 40°$.

As shown in Fig. 1, beyond 20–25 m/s depending on incidence angle, the NRCS given by the CMOD5.N tends to be saturated, while that calculated by the SSA and RCA still increases with wind speed. This evokes the idea about the use of EM GMF to estimate high or extreme wind speed.

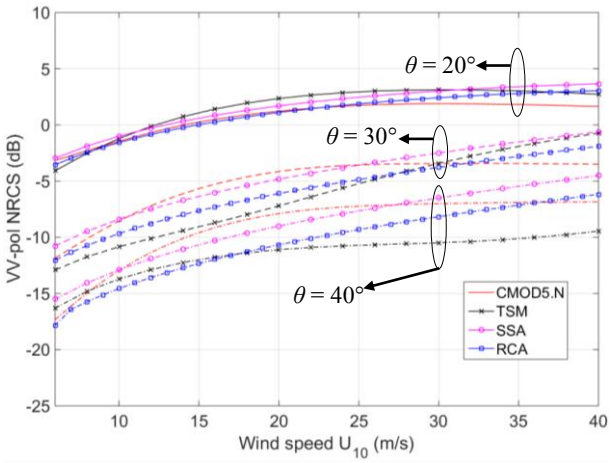

(a)

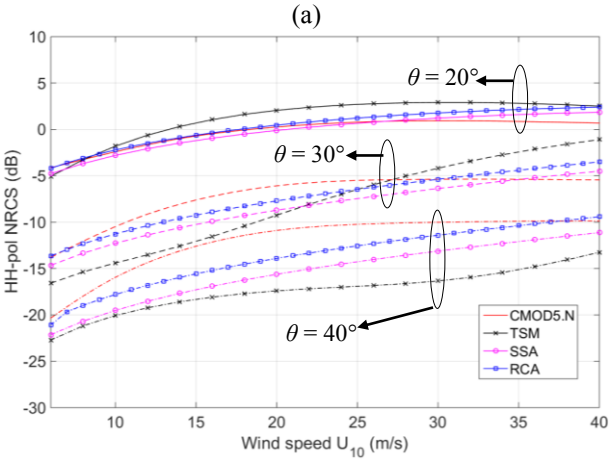

(b)

Figure 1. Comparison of NRCS calculated by the CMOD5.N [6], CTSM [9], SSA [10], and RCA [11] for up-wind direction ($\Phi_{re} = 0°$) in (a) VV-pol and (b) HH-pol. The surface roughness spectrum studied with the CTSM, SSA, and RCA is proposed by Hwang [14] (omnidirectional part) and McDaniel *et al.* [15] for the angular spreading function.

4. Wind Speed Estimation

We present in Fig. 2 the estimated wind speed by the CMOD5.N and RCA from a Sentinel-1 image acquired in HH-pol and with SM (StripMap) mode (80 km swath width). The obtained results with the CTSM and SSA are not presented here since the NRCS calculated by them is overestimated as shown in Fig. 1. In general, the estimated wind speed by the CMOD5.N and RCA is very close (2 m/s maximum difference). This has been expected from Fig. 1b for $\theta = \sim 35°–40°$. Wind directions shown in Fig. 2 are extracted by the Local Gradient (LG) method [16]. They are also used for the RCA to estimate wind speed. In order to obtain high-resolution and accurate wind fields at the scale of 2.5 km, the dimension of original image with a pixel size of 10 m (or 250 pixels for a 2.5-km wind cell) is reduced with the ratio of 1:10. It means that a 2.5-km wind cell of the size-reduced image contains 25 pixels.

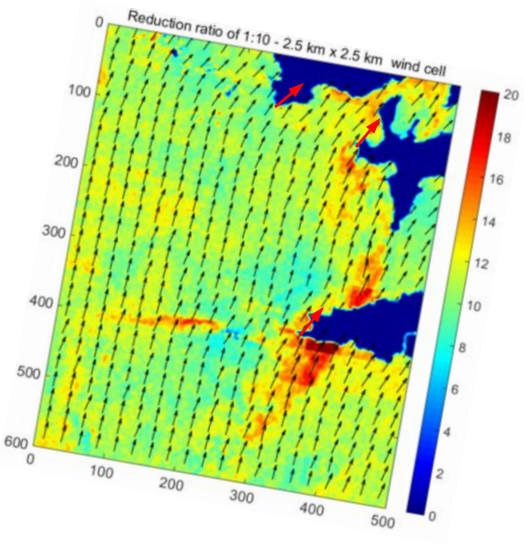

(a)

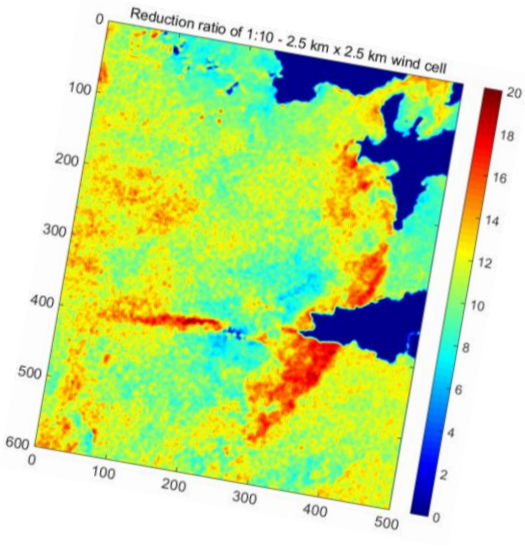

(b)

Figure 2. Estimated wind field at the scale of 2.5 km from a Sentinel-1 image acquired on Nov. 2, 2014 in HH-pol and with SM mode (ID #C244). (a) Wind direction extracted by the LG method [16] + wind speed estimated by the CMOD5.N [6]. (b) Wind speed estimated by the RCA [11].

5. Conclusion and Perspectives

We present in this paper the application of EM models for near-surface wind speed retrieval in C-band. In general, despite based on different approaches, the EP and EM models give quite similar NRCS, especially for $\theta < 40°$. Likewise, the estimated wind speed by the EP GMF (CMOD5.N) and EM GMF (SSA for VV-pol, RCA for HH-pol) is very close. However, for $\theta > 40°$ the NRCS calculated by the EM models is smaller than that of the CMOD5.N. The reason is that the contribution of wave breaking and foam to NRCS has not been taken into account in the description of EM models. This should be considered in the next steps to improve the performance of the NRCS calculation of EM models. For high and extreme wind speed (above 25 m/s), the NRCS calculated by the CMOD5.N tend to be saturated, while that given by the EM models still increases with wind speed. This evokes the possibility of EM models for the estimation of extreme winds.

6. Acknowledgements

This work is supported by Direction Générale de l'Armement (DGA) in the frame of the SIMUSO project. The authors would like to thank to Dr. H. Ghanmi for the discussion of electromagnetic models.

7. References

1. A. A. Mouche, F. Collard, B. Chapron, K-F. Dagestad, G. Guitton, J. A. Johannessen, V. Kerbaol, M-W. Hansen, "On the Use of Doppler Shift for Sea Surface Wind Retrieval From SAR," *IEEE Trans. on Geo. & Rem. Sens.*, **50**, 7, Jul. 2012, pp. 2901–2909, doi: 10.1109/TGRS.2011.2174998.

2. A. Montuori, P. de Ruggiero, M. Migliaccio, S. Pierini, G. Spezie, "X-band COSMO-SkyMed wind field retrieval, with application to coastal circulation modeling," *Ocean Sci.*, **9**, Feb. 2013, pp. 121–132, doi: 10.5194/os-9-121-2013, 2013.

3. A. Stoffelen, D. Anderson, "Scatterometer data interpretation: Estimation and validation of the transfer function CMOD4," *J. Geophys. Res.*, **102,** C3, Mar. 1997, pp. 5767–5780, doi: 10.1029/96JC02860.

4. Y. Quilfen, B. Chapron, T. Elfouhaily, K. Katsaros, J. Tournadre, "Observation Of tropical cyclones by high-resolutions scatterometry," *J. Geophys. Res.*, **103**, C4, Apr. 1998, pp. 7767–7786, doi: 10.1029/97JC01911.

5. H. Hersbach, A. Stoffelen, S. De Haan, "An improved C-band scatterometer ocean geophysical model function: CMOD5," *J. Geophys. Res.*, **112**, C3, Mar. 2007, pp. C03006, doi: 10.1029/2006JC003743.

6. H. Hersbach, "CMOD5.N: A C-band geophysical model function for equivalent neutral wind," *ECMWF Reading*, U.K., 2008. Tech. Memo. 554.

7. A. Colliander, P. Ylä-Oijala, "Electromagnetic Scattering From Rough Surface Using Single Integral Equation and Adaptive Integral Method," *IEEE Trans. on Ant. & Prop.*, **55**, 1, Dec. 2007, pp. 3639–3646, doi: 10.1109/TAP.2007.910337.

8. D. Holliday, L. L. DeRaad, , G. J. St-Cyr, "Forward-Backward: A new method for computing low-grazing angle scattering," *IEEE Trans. on Ant. & Prop.*, **44**, 5, Aug. 2002, pp. 722–729, doi: 10.1109/8.496263.

9. A. Khenchaf, "Bistatic scattering and depolarization by randomly rough surface: Application to natural rough surface in X-band," *Wave in Random and Complex Media*, **11**, 2, Aug. 2006, pp. 61–89, doi: 10.1088/0959-7174/11/2/301.

10. A. G. Voronovich, "Small slope approximation in wave scattering from rough surfaces," *J. of Experimental and Theoretical Physics*, **62**, 1985, pp. 65–70.

11. A. A. Mouch, B. Chapron, N. Reul, D. Hauser, Y. Quilfen, "Importance of the sea surface curvature to interpret the normalized radar cross section," *J. of. Geophysical Res.*, **112**, C10002, Oct. 2007, doi: 10.1029/2006JC004010.

12. J. Horstmann, W. Koch, S. Lehner, R. Tonboe, "Ocean winds from RADARSAT-1 ScanSAR," *Can. J. Remote Sens.*, **28**, 3, 2002, pp. 524–533, doi: 0.5589/m02-043.

13. G. Liu, X. Yang, X. Li, B. Zhang, W. Pichel, Z. Li, X. Zhou, "A Systematic Comparison of the Effect of Polarization Ratio Models on Sea Surface Wind Retrieval From C-Band Synthetic Aperture Radar," *IEEE J. of Selected Topics in Applied Earth Obs. & Rem. Sens.*, **6**, 3, Feb. 2013, pp. 1100–1108, doi: 10.1109/JSTARS.2013.2242848.

14. P. Hwang, "A note on the ocean surface roughness spectrum," *J. Atmos. Oceanic Technol.*, **28**, 2011, pp. 436–443, doi: 10.1175/2010JTECHO812.1.

15. S. T. McDaniel, "Small-slope predictions of microwave backscatter from the sea surface," *Wave Random Media*, **11**, 2001, pp. 343-360. doi: 10.1080/13616670109409789.

16. W. Koch, "Directional Analysis of SAR Images Aiming at Wind Direction," *IEEE Trans. on Geo. & Rem. Sens.*, **42**, 4, Apr. 2004, pp. 702–710, doi: 10.1109/TGRS.2003.818811.